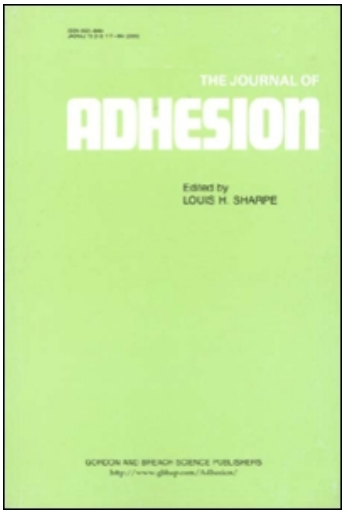

The Journal of Adhesion

Publication details, including instructions for authors and subscription information:
http://www.informaworld.com/smpp/title~content=t713453635

Underwater Adhesion Measurements using the JKR Technique

Carl Loskofsky[a]; Feng Song[a]; Bi-min Zhang Newby[a]
[a] Department of Chemical and Biomolecular Engineering, The University of Akron, Akron, Ohio, USA

To cite this Article Loskofsky, Carl , Song, Feng and Newby, Bi-min Zhang(2006) 'Underwater Adhesion Measurements using the JKR Technique', The Journal of Adhesion, 82: 7, 713 — 730
To link to this Article: DOI: 10.1080/00218460600775807
URL: http://dx.doi.org/10.1080/00218460600775807

The Journal of Adhesion, 82:713–730, 2006

ISSN: 0021-8464 print/1545-5823 online
DOI: 10.1080/00218460600775807

Taylor & Francis
Taylor & Francis Group

Underwater Adhesion Measurements using the JKR Technique

Carl Loskofsky
Feng Song
Bi-min Zhang Newby
Department of Chemical and Biomolecular Engineering,
The University of Akron, Akron, Ohio, USA

The JKR (Johnson–Kendall–Roberts) method of contact mechanics has been widely utilized for measuring adhesion properties between a deformable elastomeric lens and various materials. Such measurements are normally performed in air. We attempted to verify whether the JKR technique could be practical for evaluating adhesion properties under water. After modifying the common JKR apparatus to be suitable for underwater studies, two types of hydrophobic coating systems, silicone/silicone and silicone/silanized silicon wafer, were used. The work of adhesion (W_A) values obtained from loading measurements and under zero load were found to be slightly smaller than the values estimated using surface energies and contact angles of water formed on the surfaces of these coatings. One possible cause for the slightly smaller values could be contamination/alteration of the coating surface properties upon immersion in water. The results suggested that, with proper control of experimental conditions, the JKR technique could be extended to evaluate adhesion properties under water.

Keywords: Bioadhesion; Silanized surfaces; Silicone elastomer; Underwater adhesion; Underwater JKR; Water contact angle

INTRODUCTION

Techniques suitable for underwater adhesion measurements are essential for understanding adhesion phenomena in aqueous environments. Some of these phenomena include fouling/antifouling, protein adsorption, blood coagulation, and cell adhesion. For example, in

Received 23 September 2005; in final form 17 April 2006.
Address correspondence to Bi-min Zhang Newby, Department of Chemical and Biomolecular Engineering, The University of Akron, Akron, OH 44325-3906, USA. E-mail: bimin@uakron.edu

antifouling, evaluating properties of coatings under water is critical. When foul-release coatings (generally hydrophobic and having low surface energy) [1] are exposed to water, because of their hydrophobic nature, the interfacial energy between the coating and water can become large, leading to a larger work of adhesion (W_A) or adhesion energy (G) as compared to their corresponding values in air. Commonly, properties of submerged coatings are evaluated via the post-submersion evaluation method, in which the coating is removed from its aqueous medium, dried, and then examined. Once removed from the aqueous environment, relevant information could be lost or altered. Therefore, to best evaluate an underwater coating, it should be assessed while submerged in water, and a simple but adequate method for such evaluations is needed.

The JKR (Johnson–Kendall–Roberts) method of contact mechanics has been widely employed for measuring adhesion properties between a deformable elastomeric lens and various materials. Johnson, Kendall, and Roberts used this technique to measure the interfacial energy between rubber and water in their seminal paper on the technique [2]. Chaudhury and Whitesides have also used the JKR technique to determine the work of adhesion between two identical surfaces under a liquid in their first set of JKR experiments [3]. The method was later applied for monitoring the adsorption of nonionic surfactants onto a solid surface under an aqueous solution [4]. Therefore, it has potential for evaluating adhesion properties of materials under water.

In this study, we attempted to construct a simple but adequate apparatus design that allows loading and unloading measurements under water to be performed. The under water work of adhesion between elastic silicone lenses and some nonpolar coatings with low surface energies were obtained from the JKR measurements and used to verify if the design and the JKR technique could be practical for evaluating adhesion properties under water.

THEORETICAL BACKGROUND

The theory behind the JKR technique has been well established [2,3,5–8]. Briefly, when two perfect elastomeric bodies are brought into contact under a certain load, Johnson, Kendall, and Roberts proposed that the energy associated with such a deformation involved the mechanical energy and surface interaction energy (G). The expression correlating the deformation (a, the radius of contact), load force (P),

and G is presented as

$$a^3 = \frac{R}{K}\left(P + 3\pi GR + \left[6\pi GRP + (3\pi GR)^2\right]^{1/2}\right) \tag{1}$$

where K is the elastic modulus of the system, which is related to the moduli and Poisson ratios of the elastic bodies. For a system like ours, where a hemispherical silicone lens is in contact with a flat elastic surface, R is the radius of curvature of the hemispherical lens. When the system reaches equilibrium, G equals the thermodynamic work of adhesion (W_A) of the two contacting surfaces. The value of W_A can be obtained from the loading measurements or from the deformational contact radius under zero load, $a_o (W_A = Ka_o^3/6\pi R^2)$. For the former, Equation (1) is arranged into a linear form and used to analyze the experimentally measured values of a and P in a linear plot following Equation (2):

$$\frac{a^{3/2}}{R} = \frac{1}{K}\left(\frac{P}{a^{3/2}}\right) + \left(\frac{6\pi W_A}{K}\right)^{1/2} \tag{2}$$

Equation (1) can also be rearranged to obtain the instant energy, $G(t)$, that arises from the interactions between the two contacting surfaces:

$$G(t) = \frac{\left([Ka(t)^3/R] - P(t)\right)^2}{6\pi Ka(t)^3} \tag{3}$$

where $a(t)$ and $P(t)$ are the instant contact radius and interaction force, respectively.

Based merely on the thermodynamics, W_A for two contacting surfaces (1 and 2) in a medium (m) can also be estimated from the interfacial energies as [9,10]

$$W_A = \gamma_{1m} + \gamma_{2m} - \gamma_{12} \tag{4}$$

where γ_{ij} is the interfacial energy at the interface of i/j. When the medium is air (v), in most cases, the surface energy of a substance (γ_i) can be used interchangeably with γ_{iv}, the interfacial energy of the substance and air. The interfacial energy of a surface immersed in water (γ_{iw}) can normally be estimated from the contact angle of water formed on the surface using the Young's equation [11]:

$$\gamma_{iw} = \gamma_{iv} - \gamma_{wv}\cos\theta_{wi}. \tag{5}$$

If only the dispersive interaction between the two surfaces (*e.g.*, silicone–silicone or silicone–hydrocarbon/fluorocarbon) exists, W_A in air can be obtained with [9,12,13]

$$W_A(=\gamma_{1v}+\gamma_{2v}-\gamma_{12})=2(\gamma_{1v}\gamma_{2v})^{1/2} \tag{6}$$

and the interfacial energy between surfaces 1 and 2 can be estimated from

$$\gamma_{12}=\gamma_{1v}+\gamma_{2v}-2(\gamma_{1v}\gamma_{2v})^{1/2} \tag{7}$$

As a result, the underwater work of adhesion for two nonpolar surfaces can be determined by combining Equations (4), (5), and (7):

$$W_A=-\gamma_{wv}\cos\theta_{w1}-\gamma_{wv}\cos\theta_{w2}+2(\gamma_{1v}\gamma_{2v})^{1/2} \tag{8}$$

When the lens and the coating are made of identical materials (1 = 2), Equation (8) can be further simplified to

$$W_A=2(\gamma_{1v}-\gamma_{wv}\cos\theta_{w1}). \tag{9}$$

EXPERIMENTAL

Materials

Experiments were performed with Sylgard® 184, an elastomeric silicone manufactured by Dow Corning Midland, MI, USA. Si wafers purchased from Silicon Quest International (Santa Clara, CA, USA) were used as supporting substrates. Deionized ultrafiltered (DIUF) water from Fisher (Bridgewater, NI, USA) was used as the liquid medium. Perfluorodecyl-1*H*,1*H*,2*H*,2*H*-trichlorosilane (FTS) and decyltrichlorosilane (DTS) from Gelest (Morrisville, PA, USA) were used to modify the Si wafers [P(100) test wafer]. ACS reagent-grade toluene, hydrogen peroxide (H_2O_2, 30% technological grade), sulfuric acid (H_2SO_4, 98%), and mineral oil were purchased from Sigma-Aldrich (St. Louis, MO, USA) and used as received.

Lens and Coating Preparation

The silicone mixture was prepared according to the manufacturer's recipe. The silicone elastic lenses were prepared by placing small drops of the mixture on a FTS-modified Si wafer. The resulting lenses had radii of curvature of 1 to 1.5 mm. Silicone coatings were prepared by spreading a small amount of silicone mixture onto a piece of Si wafer (2 cm × 2 cm) using a Doctor blade, and on average, the coating had a thickness $\sim$0.5 mm. Lenses and coatings were cured at room temperature, 100°C and 150°C for 48 h, 1 h, and 20 min, respectively. They were then soaked in ACS-grade toluene for 20 h and thereafter extensively rinsed with fresh toluene to

remove any loose silicone chains. The extracted lenses and coatings were stored inside a glass Petri® dish for at least 48 h prior to contact angle and JKR measurements. Each curing condition was found to result in coatings with a certain degree of contact-angle hysteresis. The silane-modified Si wafers (referred as the silanized Si wafer) were prepared by exposing freshly cleaned (using 30 v.%/70 v.% H_2O_2 and 98% H_2SO_4 solution) and oxidized (UV/O oxidation for 6 min) Si wafers to a mixture of FTS/DTS (10/90 by volume) vapor inside a desiccator at a reduced pressure ($\sim$25 mTorr) for 30 min [3,14,15]. The vapor was generated from 200 µl of the silane mixture in 3 g of mineral oil. The modified samples were sonicated in toluene for 5 min and then thoroughly rinsed with toluene to remove unreacted silane molecules.

JKR Apparatus for Underwater Measurements

The adhesion between a hemispherical silicone lens and a flat coating was evaluated in air and under DI water using the JKR setup sketched in Figure 1. A zigzag-shaped glass lens holder was

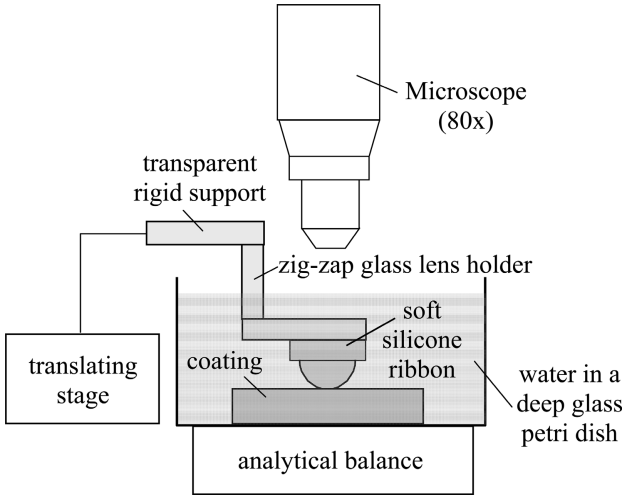

FIGURE 1 Sketch representation of JKR setup to obtain W_A and G during loading and unloading measurements respectively. When measurements were conducted under water, the Petri® dish was filled with DI water to ensure that the liquid level was high enough to submerge the lens and some portions of the lens holder figure (sketch not to scale).

constructed with the vertical plate perpendicular to both horizontal plates, and the exact dimension and surface chemistry of the vertical plate were determined prior to measurements. To eliminate the discontinuity of the elasticity, a thin ribbon was placed in between the elastic lens and the lower horizontal plate, thus modifying the set up of Deruelle *et al*. [6]. DIUF water was held inside a glass Petri® dish, and to eliminate water evaporation, a clear plastic wrap was used to seal the opening of the Petri dish. The lens holder (precleaned and prewetted before each use) was allowed to enter the dish through a small opening in the wrap (large enough to ensure the holder did not touch the edges of the opening). A glass sample stage was secured to the bottom of the Petri dish, and the silicone on Si wafer or silanized Si wafer was attached to the stage using a piece of double-sided tape. The level of water was at least 1 cm above the lower flat plate of the lens holder to eliminate any force that could be exerted on the holder during the advancing or retracting of the holder.

The water evaporation rate was monitored as well, and it usually turned out to be very small (*i.e.,* 0.3–0.5 mg/min over $\sim$10 min for an entire loading and unloading run) as compared with the load (P: -200 to 1200 mg). The force (*e.g.*, capillary force) exerted on the vertical plate (with a horizontal perimeter of $\sim$12 mm) while it was traveling up and down in water was also calibrated. Because the plate was prewetted and the incremental distance that the plate traveled vertically was $\sim$10 μm, the total force acting on the plate was likely minimal. As the plate was pushed down (or pulled out), a positive (or negative) force ($\sim$20 mg) resulted, and the force decreased to a value of $<$5 mg at the end of the 30-s waiting time. This force was small compared with the incremental loading (or unloading) force of $\sim$200 mg; therefore, it was not taken into account for each measurement, and instead was only considered as a part of the measurement error.

JKR Measurements

First, the contact area under zero load was determined. To achieve this, the hemispherical silicone lens was held by a high-precision-tip tweezer (TDI International, Inc., Trecsou, AZ, USA) and gently placed onto the coating surface under water. Air bubbles were sometimes adhered to the hydrophobic coating and/or lens immersed in water, and when contact was made, the air formed a "ring" of gas around the contact. The adhered air needed to be removed prior to making a proper contact. The area of contact was magnified *via* a 4$\times$ objective connected to an infinity tube portable microscope video system (a total

magnification of 80×, from Edmund Scientific, Barrington, NJ, USA). Images were taken *via* the Dazzle Digital Imaging and its software. The diameter of the contact area was measured with Scion imaging software (Scion Corporation, downloaded free from www.scioncorp.com). To determine the time required to reach equilibrium during the loading and unloading steps, the lens was held in contact with the coating at a particular contact area after a loading or unloading increment, and the variations of force and contact area were recorded. The interaction force was measured *via* an analytical electronic balance with an accuracy of 0.1 mg. Both contact area and force were recorded every 10 s up to 60 s, then every minute up to 5 min, and finally every 5 min up to ~60 min. During the consecutive loading and unloading measurements, the lens was brought into contact with the coating, and the contact area and the interaction force were taken 30 s after each loading or unloading step. No additional procedures were devoted to avoid contamination of the DIUF water during all measurements.

A contact-angle goniometer (model 100-00, Rame-Hart, Inc., Mountain Lakes, NJ, USA) was used to measure the contact angles of water and hexadecane on the coating in air. With hexadecane on silicone, the measurement was performed within 15 s of forming the drop to reduce the swelling and surface alteration of silicone.

RESULTS AND DISCUSSION

The main focus of this study is to verify the validity of the JKR technique, especially during loading, for underwater adhesion measurements; therefore, only nonpolar surfaces were used to reduce complications that may arise from the polar interactions between the surface and the highly polar water. The surfaces included one silanized Si wafer and three pure silicones. The pure silicones were Sylgard® 184 cured differently to have different modulus and water contact angles. For a silicone lens in contact with one of the surfaces, the underwater work of adhesion measured *via* the JKR technique (both under zero load and with loading measurements) was compared with the value estimated using Equation (8) or Equation (9), and the possible reasons for discrepancy are discussed.

Contact Under Water

Because of the hydrophobic nature of the lens and coatings used in this study, air bubbles occasionally adhered to the surfaces while they were being immersed, so precautions had to be taken to remove such air

bubbles prior to making contact. Obtaining a clear image of the contact area under water between the silicone lens and the silicone coating on Si wafer was sometimes difficult. The difficulty in observing the contact area could be the result of the small difference (~ 0.1) in the refractive indices between silicone (PDMS has a refractive index of ~ 1.43) and water (refractive index ~ 1.33). Also, the plastic wrap covering the dish and the water layer (~ 1 cm in depth) above the interested region absorbed and deflected some of the light traveling back into the microscope, making clear imaging even harder. If only a Si wafer or modified Si wafer was used to make contact with the silicone lens, a clear circular contact was relatively easily obtained. For this latter case, the difference in refractive indices of the Si wafer (index ~ 3.4) and water was sufficient to bring out the contrast. In all cases, with adequate preparation, a homogenous contact area with no visible defects could be obtained, which indicated that the water at the interface was likely completely expelled and intimate contact was made [3,16]. After meeting such conditions, the contact area under zero load was measured, and the loading and unloading measurements were then conducted.

Work of Adhesion from Zero Load Contact

The work of adhesion (W_A) under a liquid can be determined from the contact area under zero external load as demonstrated by the earlier works of Chaudhury and co-workers [3,4]. These values could then be used as a validation to the values measured from loading experiments. The W_A value (under water) determined from the contact area under zero load for the silicone lens (cured at 150°C) on a flat silicone sheet (cured at 100°C) was $72 \pm 4\,\mathrm{mJ/m^2}$, which was similar to the reported values [3] and a slightly smaller but comparable with the W_A ($\sim 76\,\mathrm{mJ/m^2}$) estimated using the static water contact angle on the two silicones (Table 1). For the same silicone lens in contact with a silanized Si wafer, the value was $54 \pm 4\,\mathrm{mJ/m^2}$. This was also slightly lower than the W_A value estimated using the static contact angles ($\sim 59\,\mathrm{mJ/m^2}$). One observation worth noting is that the coatings, especially the silanized Si wafer, appeared to be contaminated or altered by the water used. In most cases, it would take 10–15 min to make a proper contact (*e.g.*, remove the adhered air bubbles) that allowed the measurement of contact area. During this period of time the coating surface was likely contaminated and/or altered to some extent.

To further verify this possibility, both the lens and the coating were submerged in water for a long period of time (~ 24 h) before contacting. A smaller contact area as compared with those only immersed in water for a short period of time (~ 10 min) was obtained; consequently, the W_A

TABLE 1 Summary of Water Contact Angles on Various Coatings and the Surface Interaction Energy (G) Values

Coating of silicone lens (150°C cured)	Water contact angles (°)			Under water		
	Advancing	Receding	Static	Loading G (mJ/m^2)	Zero load W_A (mJ/m^2)	W_A (mJ/m^2) estimated
Silicone (cured, T_{rm})*	115.6 ± 2.4	69.2 ± 3.6	103.5 ± 3.5	53.3 ± 2.9 (~76)	—	77.9 ± 8.5 [~−8]
Silicone (100°C cured)	112.2 ± 3.2	84.7 ± 1.2	103.8 ± 2.8	52.2 ± 4.5 (~75)	71.9 ± 4.1	76.5 ± 5.3 [~33]
Silicone (100°C cured) (submersed in water for ~24 h)	104.0 ± 3.0	81.5 ± 2.6	97.2 ± 2.4	—	56.0 ± 1.9	63.0 ± 5.1 [~23]
Silicone (150°C cured)	112.2 ± 2.5	86.7 ± 0.7	102.1 ± 1.5	49.6 ± 2.3 (~71)	—	74.4 ± 3.7 [~36]
Silicone (150°C cured) (submersed in water for ~24 h)	108.9 ± 2.6	81.9 ± 1.4	97.9 ± 1.8	—	—	—
Flesh silanized Si wafer	103.8 ± 3.9	90.4 ± 1.3	92.8 ± 2.5	40.6 ± 1.8 (~58)	53.8 ± 3.6	58.5 ± 5.0 [~36]
Silanized Si wafer (submersed in water for ~24 h)	92.2 ± 3.3	55.8 ± 9.6	87.2 ± 2.2	25.6 ± 1.1 (~37)	30.2 ± 4.6	46.1 ± 5.1 [~−12]

*The lens contacting this coating was also cured at room temperature.

Notes: Data were measured, using our JKR apparatus, under water between a silicone lens and a silicone coating or a silanized Si wafer. Each data point resulted from at least six measurements. The estimated W_A values, using Equation (8) and γ_{sv} of 22 and 18 mJ/m^2 for silicone and silanized Si wafer, respectively, are presented for comparison. The values inside [] were estimated from the receding water contact angles on the coatings, whereas those inside () were the possible equilibrium value (W_A) extrapolated from the measured loading G value by assuming this value was ~0.7 W_A. The average ratio (from four different sets) of the G value at a 30 s waiting time to the average of all G values in the range of 1200 s to 2400 s for the silicone lens (cured at 150°C) in contact with the silanized Si wafer (see Figure 2) was 0.7.

values were smaller. With 24 h of immersion, W_A for the silicone/silicone system was $\sim 56\,mJ/m^2$, whereas it was $\sim 30\,mJ/m^2$ for the silicone/silanized-Si-wafer system. Alterations of the coating surface with immersion, such as re-orientation of surface molecules to expose their water-liking moieties, have been reported for hydrophobic surfaces [17]. As a result, the surface energy and water contact angle on the coating changed. In addition, upon long exposure, the surfaces of the coating and the lens became more contaminated (visible deposits were observed) as a result of the adsorption/deposition of substances dissolved or dispersed in the water. These substances could be more hydrophilic in nature when compared with both the silicone and the silanized Si wafer, which could contribute to a reduction of the interfacial energy, γ_{iw}. A reduction of water contact angles (see Table 1) on the coatings after immersion was indeed observed [18], especially for the silanized Si wafer. By using the static water contact angles formed on the coatings after being immersed for ~ 24 h, the W_A value estimated ($\sim 63\,mJ/m^2$) was again slightly greater than that obtained from zero load contact for the silicone system, but the estimated value ($\sim 46\,mJ/m^2$) was $\sim 35\%$ greater than the measured value for the silicone/silanized-Si-wafer system. The lower experimentally obtained values could be due to the inaccuracy in the contact angle values measured on the postsubmerged coatings. The measurements were conducted in air with the submerged sample taken out from the water bath and dried. Because the silanized Si-wafer was contaminated more than the silicone coatings, more of the loosely deposited substances were removed as the sample was extracted from the water bath and/or blown dry leading to a greater increase in the contact angle value.

Equilibrium for Loading and Unloading Measurements

A JKR apparatus that allows loading and unloading measurements would greatly extend its usefulness. We have constructed the zigzag design to allow the loading and unloading measurements under water. Although we have attempted to minimize complications, *e.g.*, capillary force, associated with the zigzag design, any uncertainty in the design would need to be cleared. Because the surface interaction energy (G) measured under equilibrium conditions during either a loading or an unloading step should be equal to the work of adhesion of the two interacting surfaces, it could be used to validate the correctness of our apparatus design. Because of the difficulty of imaging the contact area of silicone on silicone, we chose to determine the equilibrium for a silicone lens cured at 150°C pressed against a silanized-modified Si wafer. The results are summarized in Figure 2.

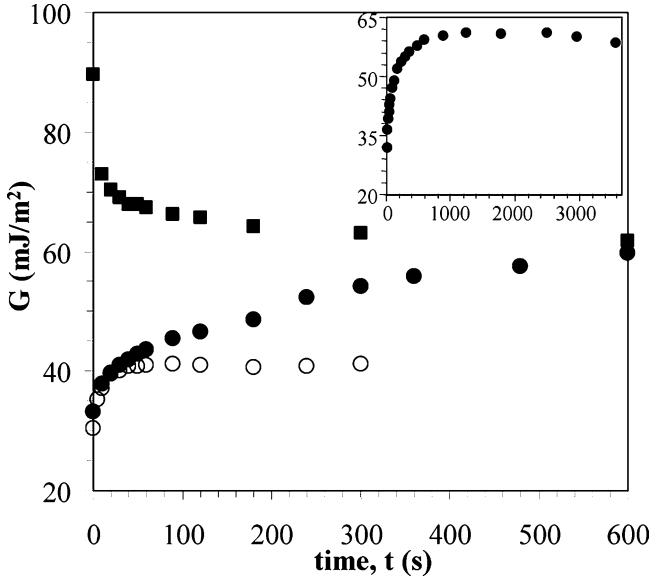

FIGURE 2 Variation of the loading or unloading surface interacting energy (G) is shown as a function of time that a silicone lens (cured at 150°C for 20 min) was held in contact with a silanized Si wafer after a particular loading or unloading step. A loading step in air and under water are represented by ○ and ●, respectively, whereas an unloading step under water is denoted by ■. The contact radius (a) after the loading step was ~174 μm for both media, whereas it was ~125 μm after the unloading step under water. The inset shows the G values after a loading step underwater for up to 1 h. After each loading step, the G value of the two contacting surfaces was less than the thermodynamic of adhesion (W_A), and thus G increased with time until equilibrium was reached (or $G = W_A$). On the other hand, after each unloading step, G was greater than W_A, and it would gradually decrease until the system reached equilibrium.

For loading studies, after each incremental loading step, we observed a rapid increase in contact area (with the resolution of our setup) within 0.3 s and 2 s, respectively, for the in-air and underwater cases. After this rapid increase, the contact area remained almost constant, but the force continued to decrease at a gradual decreasing rate until equilibrium was reached. With a similar contact area, it took 30–40 times longer to reach the equilibrium for the loading process under water as compared with that conducted in air. In air, the G value reached a plateau of ~41 mJ/m^2 in 30–40 s and remained constant, whereas for the submerged case, the value reached a maximum (~62 mJ/m^2) in ~1200 s and maintained around that value to about

2400 s, where it started to decrease slowly (see inset of Figure 2). The maximum value agreed reasonably well with the estimated W_A value ($\sim 59\,mJ/m^2$). The short time (*i.e.*, a few seconds) needed for the two interacting surfaces to reach equilibrium in air was also reported by others [5,8]. The equilibrium of loading between the lens and coatings that had been submerged under water for 24 h was also performed, and the results showed that G reached plateau values of 33–38 mJ/m^2 for different runs; the values were smaller as compared with those ($\sim 62\,mJ/m^2$) of the same lens and coating without a prolonged (< 1 h) immersion. The decrease of the maximum loading G values for the prolonged submerged coatings could be the result of surface alteration and contamination in water as mentioned earlier.

For unloading studies under water, after each unloading step the contact area decreased quickly during the first 2 s and then continued to decrease at a much slower rate, while the force continued to increase gradually. This resulted in a sharp decrease in G during the first 30 s, and then the value continued to decrease with a gradually reducing rate. The reduction rate dropped to $\sim 0.1\,mJ/m^2$-min in 10–15 min after the unloading step, at which time the G value was $\sim 62\,mJ/m^2$, the maximum G value obtained for loading in water. However, the unloading G value continued to reduce when the contact was held under water for longer times.

Loading/Unloading Measurements

Prior to running the loading and unloading measurements under water, W_A of the coatings in air, obtained from loading, was first measured and compared with both the estimated values [using Equation (6)] and the reported literature data [3,19] to illustrate that the design was adequate for loading/unloading measurements in air. Also, the modulus of each system obtained from loading in air was used later for calculating the G values under water. The waiting time for each loading step was chosen to be 30 s based on the time needed to reach equilibrium for loading in air for the silicone/silanized-Si-wafer system evaluated previously. Also, for in air measurements, the G value obtained from the intercept of the loading data curve for 30 s of waiting time was basically the same as that of 60 s or 120 s of waiting time for three systems studied (a 150°C cured silicone lens in contact with a 150°C cured silicone sheet, with a 100°C cured sheet, and with a silanized Si wafer). Our loading G values, obtained from the intercept of the loading curve, or average of all eight loading G values (one for each loading step), were close to those reported and/or estimated W_A values ($\sim 44\,mJ/m^2$ and $\sim 40\,mJ/m^2$ for silicone/silicone and

silicone/silanized Si wafer, respectively) using Equation (6). This evidenced that the apparatus was suitable for JKR measurements in air.

Because a longer time for underwater runs could lead to alterations of coating surface properties, which could complicate our data analysis, 30 s of waiting time (or $\sim$10 min for the entire loading/unloading run) for each loading or unloading step was also used for underwater runs, although such a short time may be insufficient for some systems to reach equilibrium. Under such loading conditions, the values of G ($52 \pm 4\,\mathrm{mJ/m^2}$) measured under water for the same silicone lens (cured at 150°C) against the same silicone sheet (cured at 100°C) used for the zero load study were smaller than the estimated W_A values ($69 \pm 5\,\mathrm{mJ/m^2}$) based on the static contact angles and the value ($\sim 72\,\mathrm{mJ/m^2}$) obtained under zero load. One possible reason for the small G value obtained during loading could be the mode of the water. During loading, with the lens was pressed against the coating, water initially residing in between the lens and the coating was being squeezed out and under the "receding" mode, similar to that of water during the receding contact angle measurement. As a result, receding water contact angles, instead of static angles, formed on the lens and on the coating might have to be used to estimate W_A. Based on this analogy, W_A was estimated to be $\sim 33\,\mathrm{mJ/m^2}$ for the silicone/silicone system; the value was much smaller than the measured loading G values. On the other hand, it was found from the earlier equilibrium study that the loading G value of a 30-s waiting time of a loading step reached $\sim$70% of the equilibrium value (the average of all G values obtained between a waiting time of 1,200 s to 2,400 s for the particular loading step. If considering this fact, the equilibrium G value for loading under water was predicted to be $\sim 75\,\mathrm{mJ/m^2}$, which was very close to W_A under zero load and that estimated using static angles. Therefore, the low G values obtained from loading measurements with 30 s of waiting time for each loading step could simply be the result of the system not reaching its equilibrium.

Figures 3 and 4 summarize the loading and unloading measurements of three different silicone/silicone systems. All three silicone sets were prepared with the identical Sylgard® 184 mixture; the only difference was the curing temperature/time. Set 1 was cured at room temperature for 48 h, set 2 was cured at 150°C for 20 min, and set 3 was cured at 100°C for 1 h. The slopes of the $a^{3/2}/R$ *versus* $P/a^{3/2}$ plots for room-temperature-cured coatings were higher than those of coatings cured at 150°C, indicating that the modulus of the latter system was larger (K at 150°C $\sim$2.5 MPa; whereas K at $T_{rm} \sim$0.75 MPa). Although both coatings appeared to be completely cured, the coatings cured at an elevated temperature have a higher cross-linking density

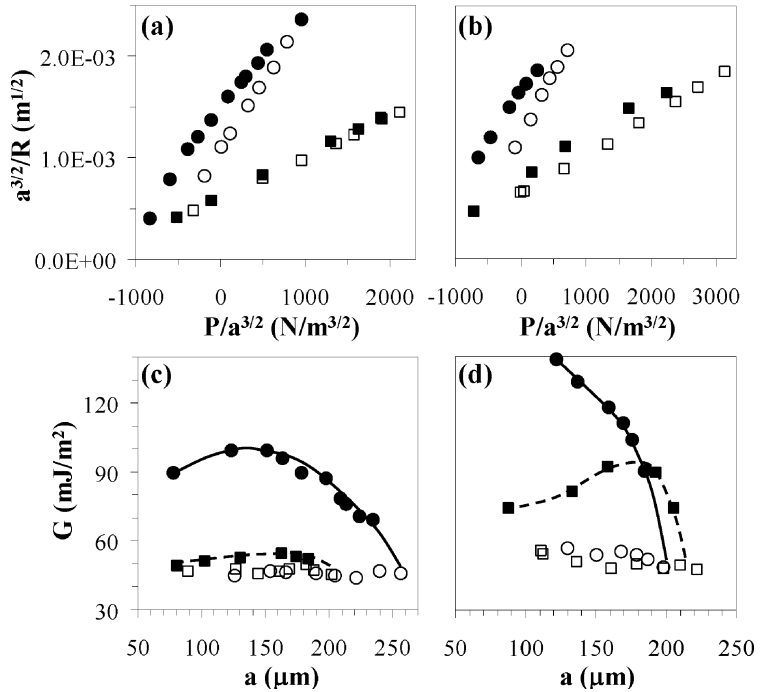

FIGURE 3 Loading (○ and □) and unloading (● and ■) data obtained in air (a) and under water (b) for a silicone hemispherical lens in contact with an ~0.5-mm coating of silicone with both cured at room temperature for 48 h (○ and ●) or 150°C for 20 min (□ and ■). Their corresponding values of loading and unloading G calculated using Equation (3) are presented, respectively, in (c) and (d). The lines are used to guide the eyes.

and behaved more like a perfect elastomer, whereas the coatings cured under room temperature exhibited certain viscoelastic behaviors. This could be the reason why a higher adhesion hysteresis (difference between the loading and unloading measurements) was noticed for the silicones (set 1) cured at room temperature (Figure 3). For set 2, the in-air unloading curve basically sat on top of the loading curve, indicating minimal hysteresis (Figure 3c).

When the measurements were conducted under water, it was first noticed that there was a slight reduction of the loading G values as the contact area increased during the loading measurements. Such a slight reduction could be the result of the longer immersion time, as a larger contact area was obtained at a later time during the loading measurements. No difference between the loading G values for

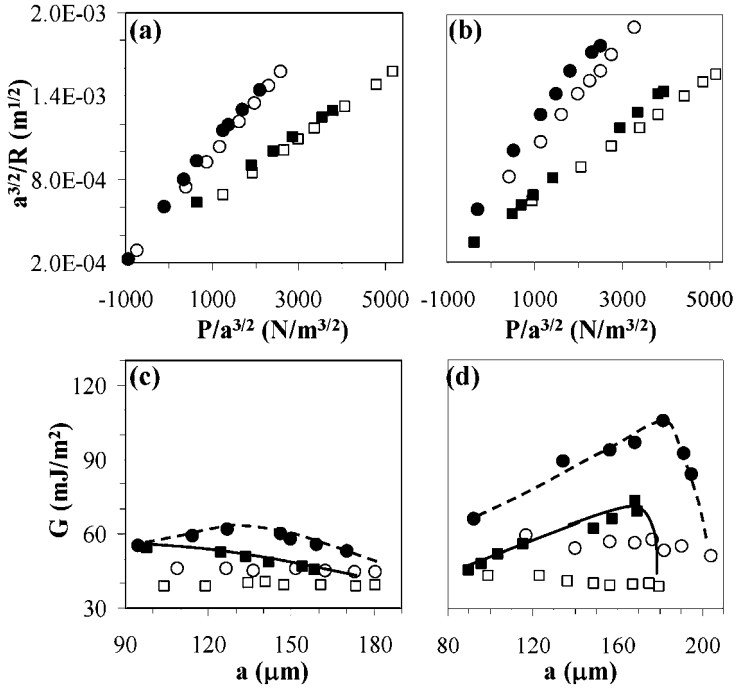

FIGURE 4 Loading (○ and □) and unloading (● and ■) data obtained in air (a) and under water (b) for a silicone hemispherical lens (cured at 150°C for 20 min) in contact with an ~500-μm coating of silicone (cured at 100°C for 1 h) (○ and ●) and with a silanized Si wafer (□ and ■). Their corresponding values of loading and unloading G calculated using Equation (3) are presented, respectively, in (c) and (d). The lines are used to guide the eyes.

coatings cured at different temperatures was observed, although the different curing temperatures resulted in noticeable difference in receding water contact angles but similar static contact angles (102–104°) on these coatings. This indicated that the underwater loading G value was likely related to the static water contact angles instead of the receding contact angle formed on the coatings. Based on the static water contact angles, the estimated W_A values for the silicone systems were 74–78 mJ/m^2. The loading G values (47–59 mJ/m^2) for runs performed within 30 min of the coatings being immersed in water and with a 30-s waiting time for each loading step were well within the expectation. Considering that such a waiting time would allow the system to reach ~70% of its equilibrium value, the equilibrium value for those loading steps would be ~67–84 mJ/m^2.

Figure 4 also shows the behaviors of a 150°C cured silicone lens compressed against and separated from the silanized Si wafer, which was used for determining the equilibrium study earlier. The loading and unloading runs in air were conducted to obtain the modulus (K) of the system and the possible adhesion hysteresis of the system. Since this silanized Si wafer was used many times for underwater studies, the coating was thoroughly cleaned and the essential surface properties (water contact angles, surface energy) were remeasured prior to the loading and unloading runs. Based on the hexadecane contact angles (52–53°) on the silanized Si wafer, the surface energy of the surface was estimated to be $\sim 18\,\mathrm{mJ/m^2}$, which resulted in the W_A value for the system to be $\sim 40\,\mathrm{mJ/m^2}$. With a waiting time of 30 s for each loading step, the range of loading G values measured in air was 38–$41\,\mathrm{mJ/m^2}$, which agreed well with the expected values. The values in water were 39–$43\,\mathrm{mJ/m^2}$, which resulted in the equilibrium values of 56–$61\,\mathrm{mJ/m^2}$. The equilibrium values were predicted by dividing the loading G values by 70% based on the equilibrium study that a 30-s waiting time resulted in the loading G value of $\sim$70% of its equilibrium value. These predicted equilibrium values of the loading JKR under water were close to the value obtained from the zero load contact and the W_A value ($\sim 58\,\mathrm{mJ/m^2}$) estimated using static water contact angle ($\sim$93°) on the silanized surface.

Although the focus of this article is on the loading studies, some interesting phenomena were also observed from the unloading measurements; the two most obvious are briefly mentioned to draw readers' attention. First, with the same contact area, most of the measured unloading G values for systems investigated were higher under water than those measured in air. Because all of the coatings and lens were highly hydrophobic, as compared to the systems in air, a larger energy could be required to separate the two hydrophobic surfaces under water because of their stronger hydrophobic attractions in water [20,21]. Second, for most silicone systems in both media (other than the room-temperature-cured ones under water), as the contact area was reduced, unloading G values appeared to reach a maximum and then drop off. This could be an indication that for the highly elastic systems, especially those cured at high temperatures (100°C and 150°C), the systems could reach the equilibrium state more quickly with a smaller contact area.

CONCLUSION

Some initial experimental results on underwater adhesion between silicone and silicone and between silicone and a silanized surface

evaluated using the JKR technique were obtained. For all the hydrophobic systems investigated, the W_A values obtained under zero loads and those extrapolated from the loading G values agreed reasonable well with the estimated W_A values based on static water contact angles formed on the coatings. The unloading G was found to be greater than the loading G for each coating system evaluated, and most of the unloading G values under water were greater than their corresponding values measured in air. With a prolonged immersion of the hydrophobic coatings in water, the loading G value or W_A between the two hydrophobic surfaces decreased. This could be attributed to the surface alteration and contamination of the coatings, and such evidences were noticed as substances deposited on the coating surface and the reduction of water contact angle of the postimmersed coatings. Nevertheless, the underwater adhesion data obtained *via* the loading measurements and under zero load were reasonably interpreted. Therefore, we believe the JKR technique is adequate for determining surface interaction energy under water. However, the proper interpretation of the underwater JKR data relies on the appropriated decoupling of the many experimental factors that could affect the measurements.

ACKNOWLEDGMENTS

Financial support from Ohio Sea Grant (Project R/MB-2) and Ohio Board of Regents (R5905-OBR) is greatly appreciated. We are grateful to Professor Manoj K. Chaudhury for many valuable discussions and Carlos A. Barrios for the initial experimental attempts. We also thank Professor Hugh R. Brown, who has also attempted to study underwater adhesion phenomena using the JKR technology and presented some of his early findings at both Adhesion Society and American Physical Society meetings in 2005, for his inspiration of this research work.

REFERENCES

[1] Brady Jr., R. F., *J. Coating Technol.* **72**, 45–56 (2000).
[2] Johnson, K. L., Kendall, K., and Roberts, A. D., *Proc. R. Soc. Lond.* Ser. A **324**, 301–313 (1971).
[3] Chaudhury, M. K. and Whitesides, G. M., *Langmuir* **7**, 1013–1025 (1991).
[4] Haidara, H., Chaudhury, M. K., and Owen, M. J., *J. Phys. Chem.* **99**, 8681–8683 (1995).
[5] Maugis, D. and Barquins, M., *J. Phys. D: Appl. Phys.* **11**, 1989–2023 (1978).
[6] Deruelle, M., Hervet, H., Jandeau, G., and Leger, L., *J. Adhes. Sci. Technol.* **12**, 225–247 (1998).

[7] Girard-Reydet, E., Oslanec, R., Whitten, P., and Brown, H. R., *Langmuir* **20**, 708–713 (2004).
[8] Leger, L. and Amouroux, N., *J. Adhes*. **81**, 1075–1099 (2005).
[9] Dupré, A., *Théorie mécanique de la chaleur* (Gauthier-Villars, Paris, 1969), p. 368.
[10] Adamson, A. W. and Gast, A. P., *Physical Chemistry of Surfaces* (Wiley, New York, 1997), 6th ed., p. 108.
[11] Young, T. in *Miscellaneous Works*, G. Peacock (Ed.) (Murray, London, 1855), Vol. 1, p. 418.
[12] Girifalco, L. A. and Good, R. J., *J. Phys. Chem.* **61**, 904–909 (1957).
[13] Fowkes, F. M., *Ind. Eng. Chem.* **56**, 40–52 (1964).
[14] Zhang Newby, B.-M., Chaudhury, M. K., and Brown, H. R., *Science* **269**, 1407–1409 (1995).
[15] Zhang Newby, B.-M. and Chaudhury, M. K., *Langmuir* **13**, 1805–1809 (1996).
[16] Microscopic air bubbles could be trapped at the interface as suggested by others [Christenson, H. K. and Claesson, P. M., *Adv. Colloid Int. Sci.* **91**, 391–436 (2001)], but with an 80× magnification used for the JKR measurements, no detectable air bubbles trapped at the interface were observed.
[17] Koberstein, J. T., *MRS Bulletin* **21**, 19–23 (1996).
[18] Barrios, C. A., Xu, Q. W., Cutright, T. J., and Zhang Newby, B.-M., *Colloids Surf. B: Biointerfaces* **41**, 83–93 (2005).
[19] Chaudhury, M. K., *J. Adhes. Sci. Technol.* **7**, 669–675 (1993).
[20] Israelachvile, J. N., *Intermolecular and Surface Forces* (McGraw-Hill, Tokyo, 1991), 2nd ed., Chap. 8, pp. 128–133, and Chap. 13, pp. 282–286.
[21] Claesson, P. M. and Christenson, H. K., *J. Phys. Chem.* **92**, 1650–1655 (1988).